Colloid Polym Sci (2007) 285:1733–1739
DOI 10.1007/s00396-007-1760-3

SHORT COMMUNICATION

Organic–inorganic nanocomposites prepared from fluoro-aramid and silica

Muhammad Ilyas Sarwar · Sonia Zulfiqar · Zahoor Ahmad

Received: 26 July 2007 / Revised: 4 August 2007 / Accepted: 9 August 2007 / Published online: 12 September 2007

Abstract Fluoro-aramid-based sol/gel-derived nanocomposites were synthesized by condensing a mixture of 4, 4′-(hexafluoro-isopropylidene)dianiline and 1,3-phenylenediamine with terephthaloylchloride (TPC) in dimethylacetamide. TPC was added in slight excess to produce amide chains with carbonyl chloride end groups and then replaced with alkoxy groups using aminophenyltrimethoxysilane to develop bonding with the silica network. Mechanical, dynamic mechanical thermal, water absorption and morphological measurements were carried out on the thin hybrid films. Increase in the tensile strength and modulus was observed as compared to pristine polyamide. The thermal decomposition temperature was found in the range of 400–500 °C. The water absorption was found to be reduced with higher silica content. The glass transition temperature and the storage moduli increased with increasing silica concentration. The maximum increase in the T_g value (345 °C) was observed with 20 wt% silica. Scanning electron microscopy revealed the uniform distribution of silica in the matrix with an average particle size ranging from 8 to 50 nm.

Keywords Aramid · Nanocomposites · Sol–gel process · Stress-strain curves · Glass transition temperature · Morphology

M. I. Sarwar (✉) · S. Zulfiqar
Department of Chemistry, Quaid-i-Azam University,
Islamabad 45320, Pakistan
e-mail: ilyassarwar@hotmail.com

Z. Ahmad
Department of Chemistry, Faculty of Science, Kuwait University,
P. O. Box: 5969, Safat 13060, Kuwait

Introduction

Polymer composite technology is expanding rapidly as progress is being made towards achieving stronger, stiffer, and low-density materials for various applications. The most important commercial materials in this area are the synthetic linear aliphatic polyamides (nylons) which are capable of being converted into fibers. It has been noted that by far, the greater part of the total output of nylons is used for fiber production, but these resins have become important in non-fibrous applications as well, particularly in engineering applications. The more complex synthetic aliphatic polyamides, which cannot be converted into fibers, have found use in adhesives and coatings. These products are known as fatty polyamides and are not generally regarded as nylons. Polyamides with at least 85% of amide group joined to two aromatic rings are known as aramids. The aramids exhibit high temperature performance and better tensile strength, but these materials may need structural modifications and reinforcements. The sol–gel chemistry [1–11] allows the incorporation of various ceramic phases that provide better options for such improvements. In our previous studies, these polymer matrices were reinforced with various ceramic phases using sol–gel process, e.g., silica [12–15], titania [16, 17], zirconia [18], boehmite [19], and colloidal silica particles [20]. A number of other such studies on reinforced hybrid materials have been reported using different ceramic phases into a variety of polymers [21–35].

The fluoro-polymers are different from the other engineering thermoplastics because their usefulness is not primarily based on their mechanical properties but rather

on the unique physical and chemical properties that result from the presence of fluorine in the polymer. The high thermal stability of the carbon fluorine bond has led to considerable interest in fluorine containing polymers as heat resistance plastics and rubber. The great diversity of applications [36] due to their unique properties includes chemical inertness, exceptional weathering resistance, excellent heat resistance and electrical insulation characteristics, non-adhesive properties, and very low coefficient of friction. The presence of fluorine atoms makes fluoro-polymers inherently non-flammable. This property enhances the value of fluoro-polymers in electrical insulation, bearing assemblies, and many electrical and mechanical devices in sensitive aerospace applications. The decomposition of fluoro-polymers can be a problem, as the resulting products can be toxic, but fortunately, the service temperatures of fluoro-polymers are quite high, ranging to 260 °C for continuous use. Most of the fluoro-polymers are obtained by chain polymerization; however, they can also be prepared by step polymerization. Fluorine substituted oligomers of 2,2-Bis (3,4-carboxyphenyl) hexafluoropropane tetraacid have been reported. It protects carbon fibers reliably from oxidation and as a binder; it can be used in combination with carbon fibers at elevated temperature for a long period of time [37].

Keeping in view the importance of fluoro-polymers, in the present study, the aramid chains were prepared from a mixture of fluoro-substituted diamine, 1,3-phenylenediamine and terephthaloyl chloride (TPC) using dimethylacetamide as a solvent. These chains were converted into carbonyl chloride end groups by adding a slight excess of TPC. This allowed the chains to be further modified with aminophenyltrimethoxysilane (APTMOS) end caps. The chemically bonded silica network was produced in situ in the matrix by hydrolysis and condensation of both tetraethoxysilane (TEOS) and APTMOS. The mechanical, thermogravimetric analysis (TGA), water absorption, dynamic mechanical thermal (DMTA), and morphological studies of these hybrid materials were investigated.

Experimental section

Materials

The monomers employed for aramid preparation include 4, 4′-(hexafluoroiso-propylidene) dianiline 98%, 1,3-phenylene diamine 99%, TPC 99% and AR-grade dimethylacetamide (DMAc) used as solvent were obtained from Aldrich. Gelest, Inc. supplied both APTMOS 99% and TEOS 98%. All these chemicals were used as received.

Preparation of nanocomposites

The condensation reaction was carried out in a flask by placing (0.05 mol) of a mixture of 4,4′-(hexafluoroisopropylidene) dianiline and 1,3-phenylene diamine under anhydrous conditions followed by the addition of 150 ml of DMAc as a solvent. After 30-min stirring, the contents of the flask were cooled to 0 °C and then 0.05 mol of TPC was added under inert atmosphere. The reaction mixture was agitated for 1 h and then allowed to attain ambient temperature. The polyamide chains were then end-capped with carbonyl chloride groups by the addition of a slight excess of acid chloride. The polymer thus prepared had an inherent viscosity of 1.37 dl/g as estimated from a solution of 0.5 g polymer in 100 ml of DMAc at 30 °C. To ensure the completion of the reaction, the reaction mixture was agitated for 24 h [38]. The chain ends were converted into APTMOS chain ends by adding stoichiometric amount of the binding agent, and stirring was continued for further 6 h that permitted bonding with the inorganic phase. For in situ generation of inorganic network, different proportions of TEOS in DMAc were mixed to the polyamide solution, and after complete mixing, a measured amount of water in DMAc was added, required to carry out the hydrolysis/condensation of TEOS into silica network in each sample. The TEOS was added in such a way so that silica contents varied from 3 to 30 wt% in the composites. The resulting reaction mixture was stirred for additional 6 h at 40 °C. Thin hybrid films from each sample containing various amounts of silica were cast by baking out the solvent in an oven at 75–80 °C. They were then soaked in distilled water to leach out any HCl produced during polymerization reaction. These films were further dried at 80 °C under vacuum for 72 h. The chemical reactions leading to the synthesis of aramid chains and formation of their subsequent nanocomposites is presented in Fig. 1.

Mechanical properties of the hybrid films with dimensions (about 14×5.0–6.8×0.25–0.35 mm^3) were studied at 25 °C with strain rate of 0.2 cm/min using an Instron universal testing instrument (model TM-SM 1102, UK). The thermal stability of the aramid and its nanocomposites were determined by a METTLER TOLEDO TGA/SDTA 851^e thermogravimetric analyzer using 1–5 mg of the sample in Al_2O_3 crucible heated from 25 to 1,000 °C at a heating rate of 10 °C/min under nitrogen atmosphere with a gas flow rate of 30 ml/min. The water absorption of aramid–silica nanocomposites were carried out according to the specifications of ASTM D570-81. The films were placed in a vacuum oven at 80 °C until the films attained a constant weight and then immediately weighed out to the nearest 0.001 g to get the initial weight (W_o). The films

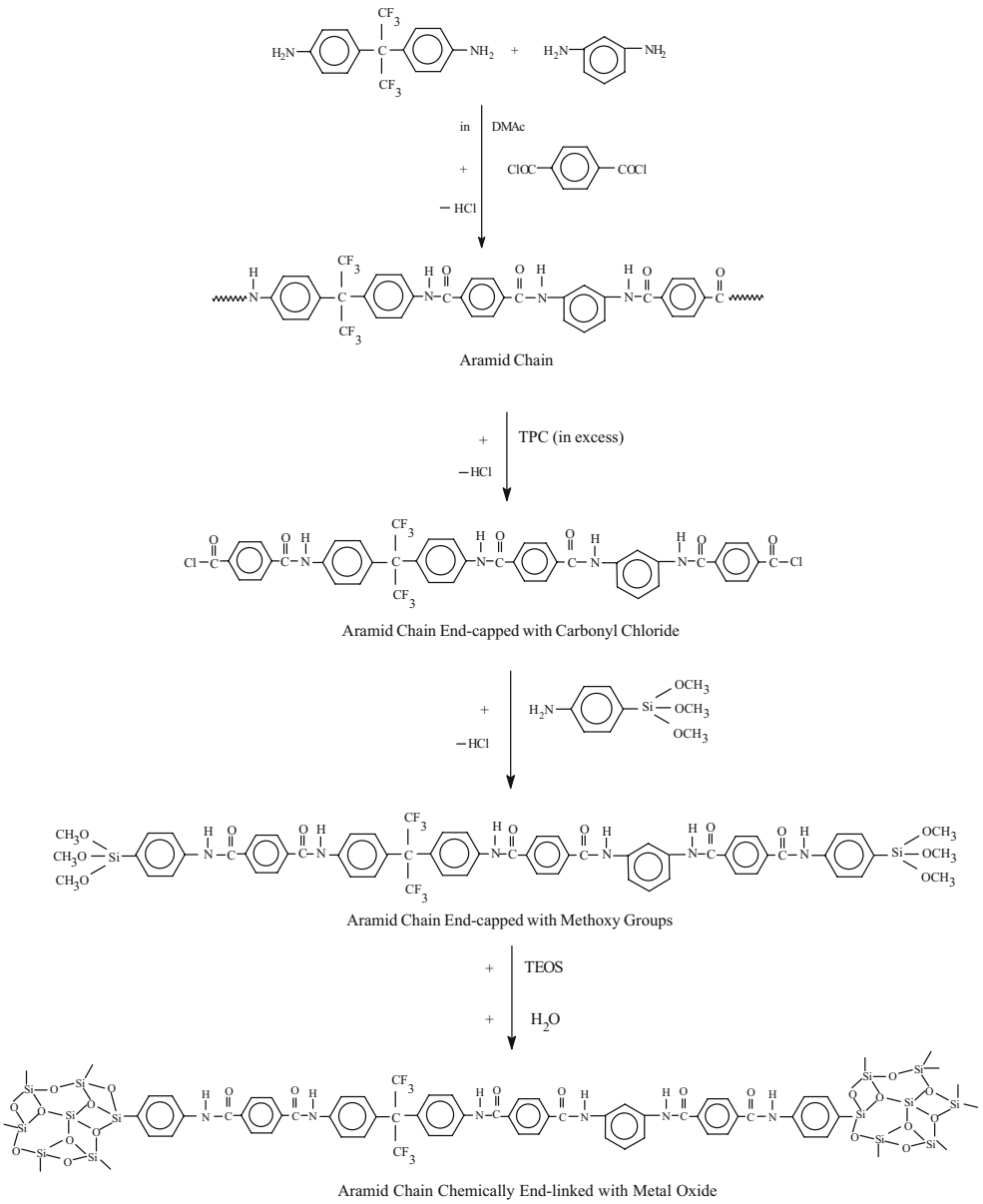

Fig. 1 Schematic synthesis of aramid and formation of its nanocomposites

were entirely immersed in a container of deionized water maintained at 25 °C. After 24 h, the films were removed from water, and then they were quickly placed between sheets of paper to remove the excess water, and films were weighed immediately. The films were again soaked in water. After another 24-h soaking period, the films were removed, dried, and weighed for any weight gain. This process was repeated again and again until the films almost attained the constant weight. The total soaking time was 168 h, and the samples were weighed at regular 24-h time intervals to get the final weight (W_f). The percentage of increase in weight of the samples was calculated to the nearest 0.01% using the formula $(W_f - W_o)/W_o$. Dynamic mechanical thermal analysis was carried out with a Rheometric Scientific DMTA III in the temperature range 40–480 °C using 10-Hz frequency. The morphology of the fractured films was investigated using a LEO Gemini 1530 microscope.

Results and discussion

The neat aromatic polyamide film was found to be transparent and gave slight tinge of brownish color. The hybrid films with 3 wt% silica were transparent, while with 7 wt% silica, it became semitransparent and light brown in

color. Beyond this concentration of inorganic phase, transparency was reduced to opaqueness. The transparency of hybrid material depends on the size, size distribution, and homogeneity of the inorganic particles in the organic phase. With higher concentrations of silica, increase in particle size and decrease in homogeneity causes opaqueness and brittleness. Mechanical properties of the pristine polyamide and hybrid films were measured at 25 °C, and average values of five and seven samples were reported in each case. The tensile strength of samples with 25 wt% or more could not be measured due to their brittleness. TGA and water absorption measurements were carried out to establish the thermal stability and water absorption behavior of these hybrid materials. DMTA and scanning electron microscopy (SEM) analyses were also performed to determine the glass transition temperature, storage moduli, and the morphology of the nanocomposites.

Mechanical properties

Stress–strain isotherms of polyamide and hybrid films with 3 to 20 wt% silica are presented in Fig. 2. The results show an increase in the tensile strength of the hybrid materials relative to the neat polyamide. The incorporation of a silica network within the polyamide phase enhances the tensile strength of the polymer. The variation in maximum stress at break (ultimate strength) as a function of silica contents is described in Table 1. A gradual increase in ultimate strength was observed. With 20 wt% silica, a maximum value of 89 MPa was obtained (relative to the 74 MPa of the neat polyamide), which indicates improvement in the tensile strength of material. The elongation at rupture (maximum strain) was found to decrease gradually with increase of silica contents. The tensile modulus was calculated from the initial slopes of the stress–strain data. The values of the modulus showed a maximum with increase in silica contents up to 20 wt% in the similar fashion as the maximum stress (Table 1).

Table 1 Mechanical and glass transition properties of fluoro-aramid/silica nanocomposites

Silica content (wt%)	Max. stress (MPa) ±0.30	Max. strain (%) ±0.02	Initial modulus (GPa) ±0.03	Toughness (MPa) ±0.50	T_g (°C)
0	74.1	29.2	1.80	53.8	306
3	79.4	20.0	1.87	38.4	–
7	86.2	16.2	1.99	31.7	325
10	87.2	13.6	2.03	26.0	332
15	88.7	9.83	2.07	17.7	338
20	89.2	9.28	2.09	17.3	345

Chemical bonding between the matrix and silica network provides reinforcement to the hybrid materials. The results indicate that if silica contents are increased beyond 20 wt%, the excess silica particles may not be linked with polymer chains, and it also increases the tendency towards particle growth. These particles may agglomerate [39]; their distribution becomes irregular and non-homogeneous, making the samples more porous and brittle. Consequently, mechanical properties of the hybrid materials reduce at higher concentrations of the inorganic phase. The toughness of these hybrid materials was measured by calculating the area under the stress–strain curves. The values of toughness decrease with addition of silica in the matrix, as does the length at break point. The results obtained on the tensile strength indicate improvement in the materials up to 20 wt%

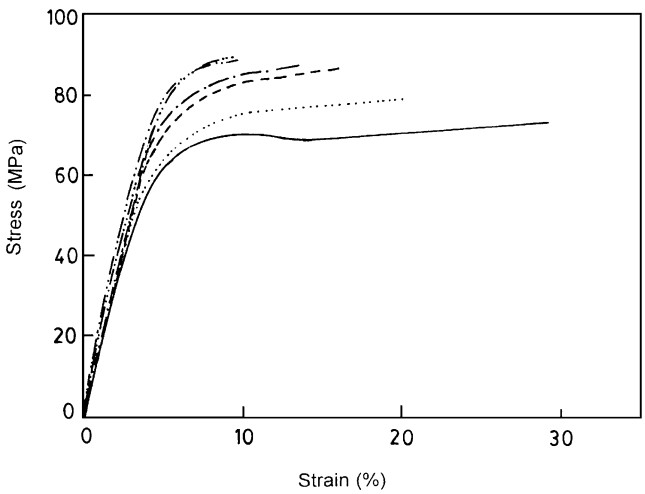

Fig. 2 Tensile strength of fluoro-aramid/silica hybrid materials; silica wt% in the matrix: 0(——), 3 (·····), 7 (— — — —), 10 (- · - · - · -), 15 (— · · — · ·), 20 (— · · · —)

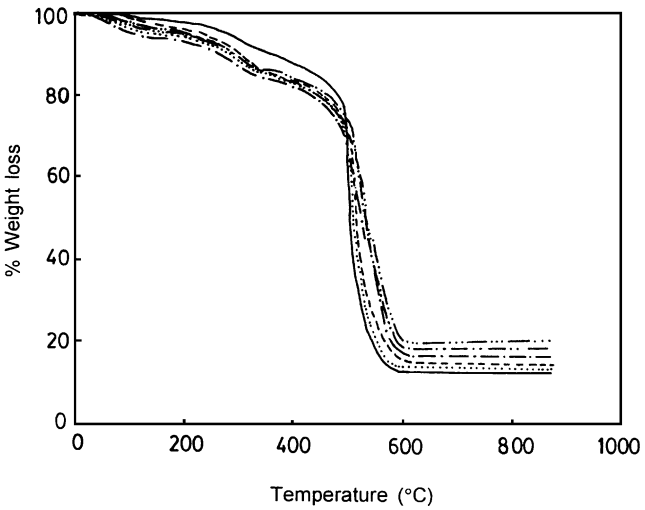

Fig. 3 TGA curves for fluoro-aramid / silica hybrid materials with different silica contents obtained at a heating rate of 10 °C/min in nitrogen; silica percent in matrix: 0 (——), 3 (·····), 7 (— — — —), 10 (- · - · - · -), 15 (— · · — · ·), 20 (— · · · —)

silica presumably due to bonding between the polymer chains and the silica, beyond which, properties undergo deterioration.

Thermogravimetric analysis

The thermal stability of composite materials with various amounts of silica was studied under nitrogen atmosphere using thermogravimetric analysis (Fig. 3). The initial change in weight is due to loss of water from some of the unhydrolyzed inorganic network. The thermal decomposition temperatures of the materials were found in the range of 400 to 500 °C, which may be mainly due to decomposition of the polymer. The weight of residue left at 800 °C was found almost proportional to the silica contents in the corresponding material.

Water absorption measurements

The amounts of water absorption of these hybrid materials measured under saturation conditions ASTM D570-81 for 168 h are presented in Fig. 4. As the polyamide chains contain polar amide groups that have the inclination to absorb water through hydrogen bonding, this measurement is important, as it can adversely affect the mechanical and dielectric properties of the hybrid materials. It was observed that the water absorption by the films consisting of pristine polyamide was maximum, i.e., 7.1%. The increase in the weight of the samples due to water absorption gradually decreased as the silica contents in the films increased. This may be due to the abundant exposure of amide groups to the surface of polymer where water molecules develop hydrogen bonding with amide groups, but as the concentration of silica is increased in the hybrid materials, the extent of water absorption at saturation point is considerably reduced. It may be due to the mutual physical interaction between the organic and inorganic phases. This interaction results in lesser availability of amide groups to interact with water. It was quite noteworthy to depict here that the progression of silica amount had no direct relationship with the decrement of extent of water absorption.

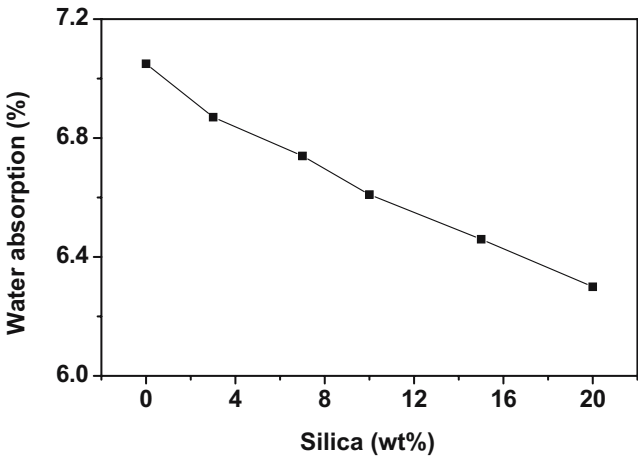

Fig. 4 Water absorption studies of fluoro-aramid/silica hybrids at equilibrium

Dynamic mechanical thermal analysis

DMTA was carried out on the neat aramid and aramid–silica nanocomposites having various amount of silica content in the temperature range of 40–480 °C. They include loss tanδ and storage modulus in bending mode. Figure 5 shows the variation of the loss tanδ with temperature for pure aramid and its composites. It is evident from the figure that with an increase in temperature, a stage is reached when the onset of segmental motion starts, as marked by a sharp rise in tanδ. In the case of pure aramid, a sharp peak is observed at 306 °C, while in the case of hybrids, the peak shifts to a higher temperature; in addition, it splits up into two parts, showing a maxima and a shoulder at still higher temperature. These peaks correspond to the α-relaxation temperatures associated with glass transition temperatures for these materials. The greater interactions between the polymeric and inorganic phases generally result in an increase in T_g. Furthermore, the intensity of the peaks decreases and become broader with higher amount of silica content, restricting the motion of the polymer chains, thereby resulting in higher T_g. The change in T_g as a function of silica content is given in Table 1. The T_g values change from 306 °C for pure aramid to 345 °C for nanocomposite with 20 wt% silica content. The behavior can be explained in terms of reduced segmental motion of the chains due to the introduction of silica network at molecular level. The addition of silica

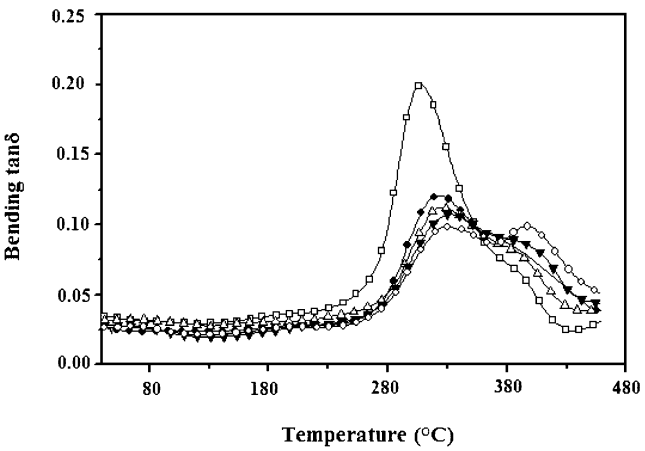

Fig. 5 Variation of loss tangent (tanδ) with temperature for fluoro-aramid/silica nanocomposites at 10 Hz, silica wt% in the matrix: 0 (*open square*), 7 (*filled circle*), 10 (*open triangle*), 15 (*filled inverted triangle*), 20 (*open circle*)

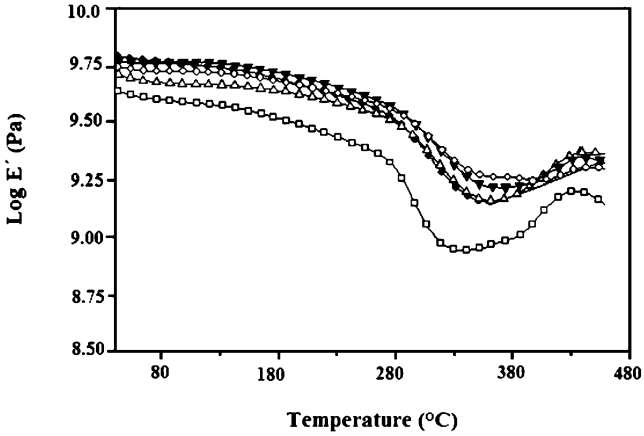

Fig. 6 Temperature dependence of storage modulus for fluoro-aramid/ silica nanocomposites at 10 Hz; silica wt% in the matrix: 0 (*open square*), 7 (*filled circle*), 10 (*open triangle*), 15 (*filled inverted triangle*), 20 (*open circle*)

shifts the peaks to higher temperature because the inorganic network hinders segmental motion of the polymer chains.

The temperature variation of storage moduli for this system is shown in Fig. 6. The storage modulus initially increases with increase in silica content, and then slightly decreases. The initial increase may be due to the completion of the condensation process leading to nearly complete network formation. The storage moduli increase with increase in silica content at a given temperature. The increase in moduli can be due to inorganic network, which has less free volume and is less flexible as compared to organic phase. However, beyond a certain limit, the inorganic structure tends to agglomerate into larger particles. This porous structure has less cohesion with the organic matrix, which results in a low modulus. The sharp decreases in modulus with onset of thermal motions are seen to occur at higher temperatures. The value of the modulus beyond 400 °C is seen to increase again with temperature possibly due to increases in cross-linking. The TGA results presented in the Fig. 3 show that the aramid chains begin to decompose around 400 °C, and this may produce free radicals which could result in increased cross-linking. At constant temperature, increasing the amounts of the silica generally increases the storage modulus because of silica's hardness and small free volume. This simple dependence can be complicated, however, by the fact that beyond a relatively low concentration of silica, there are no longer any reactive polymer ends left for the desired interfacial bonding.

Scanning electron microscopy

The morphology of the fractured surfaces of fluoro-aramid/ silica nanocomposite films was investigated using SEM to find out the distribution of silica in the hybrid materials. The micrographs of the hybrid materials with 7, 10, 15 and

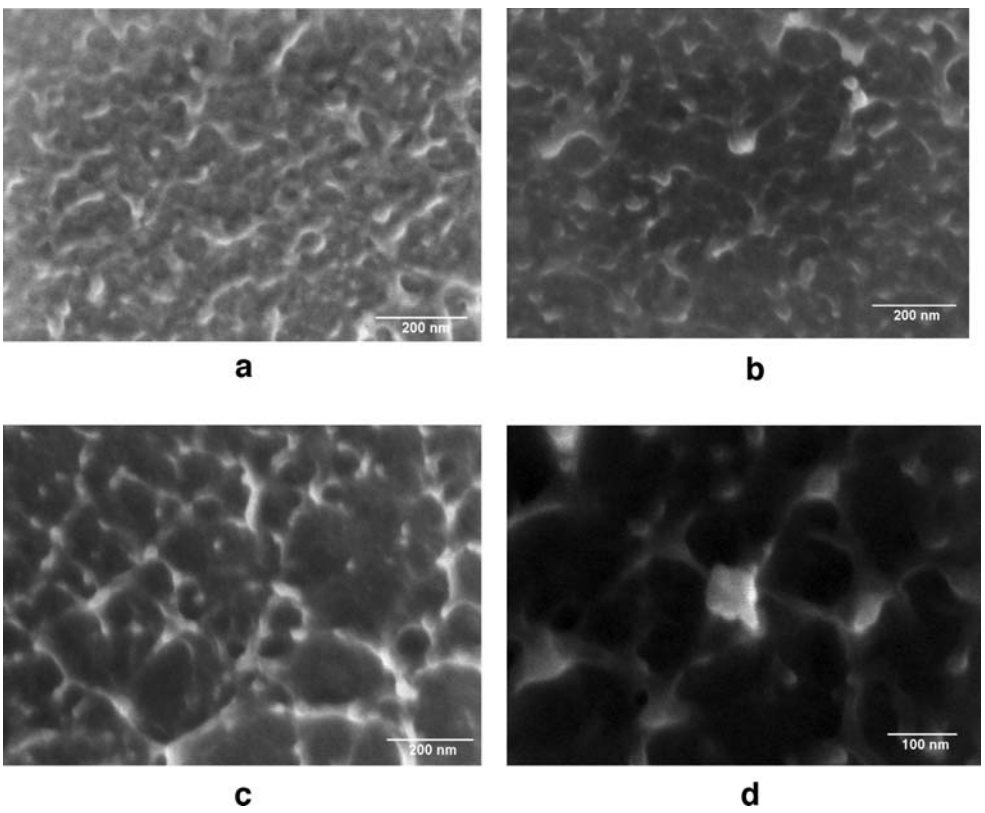

Fig. 7 Scanning electron micrographs of nanocomposites, silica content: **a** 7; **b** 10; **c** 15; and **d** 20 wt%

20 wt% of silica in the matrix are represented in Fig. 7. The particle sizes within the hybrid films prepared by sol–gel process are ranging from 8–50 nm. This demonstrates that nanocomposites can be prepared using the same technique. The micrographs clearly show a fine interconnected or co-continuous morphology. This phenomenon also reveals that the silica network have rough surfaces and diffused boundaries, giving co-continuous morphology with a better interfacial cohesion that improve the efficiency of stress transfer mechanism between the two components. In spite of the enhanced cohesion, the elongation at break decrease since the interconnected silica phase hinder the plastic flow of the polyamide phase, preventing large deformation to occur before fracture. In addition, the better compatibility between smaller silica nanoparticles and the aramid in the nanocomposite films result in improved tensile strength. An increase in silica concentration increases the particle size, and these large domain sizes can result in light scattering of silica contents, giving opaqueness to the hybrids. Therefore, these results are in accordance with the physical properties measured with different silica concentration of composite films.

Conclusions

Mechanically strong and thermally stable fluoro-aramid/silica nanocomposite materials were successfully prepared through the sol–gel process. The chemical bonding between the organic and inorganic phases provides reinforcement in the materials and is reflected in the mechanical properties. However, only appropriate amounts of both the phases give better interactions, and in the present case, an optimum tensile strength observed (89 MPa) with 20 wt% silica content in the polyamide matrix. The amount of water absorption is reduced with the addition of inorganic network. The glass transition temperature and the storage moduli determined indicate the better cohesion between the disparate phases. The shift in the T_g values suggests the interaction between the two phases. The morphological investigations indicate a narrow size distribution of silica particles in the aramid matrix. These thermally stable hybrid materials may also act as matrices for fiber reinforced composites for aerospace applications.

Acknowledgments Special thanks are due to Professor Dr. Gerhard Wegner and Dr. Ingo Lieberwirth of Max Planck Institute for Polymer Research, Mainz, Germany, for providing the SEM measurement facility.

References

1. Brinker CJ, Scherer GW (1990) Sol–gel science: the physics and chemistry of sol–gel processing. Academic, Boston
2. Hench LL, West JK (1990) Chem Rev 90:33
3. Mark JE (1992) J Appl Polym Sci Appl Polym Symp 50:273
4. Mark JE (1993) J Inorg Organomet Polym 1:431
5. Schmidt H (1994) J Sol Gel Sci Technol 1:217
6. Betrabet SC, Wilkes GL (1994) J Inorg Organomet Polym 4:343
7. Schmidt H, Kasemann R, Burkhart T, Wagner G, Arpac E, Geiter E (1995) ACS Symp Ser 585:331
8. Mascia L (1995) Trends Polym Sci 3:61
9. Gaw K, Suzuki H, Kakimoto M, Imai Y (1995) J Photopolym Sci Technol 8:307
10. Kita H, Saiki H, Tanaka K, Okamoto K (1995) J Photopolym Sci Technol 8:315
11. Mark JE, Wang S, Ahmad Z (1995) Macromol Chem Symp 98:731
12. Wang S, Ahmad Z, Mark JE (1993) Polym Bull 31:323
13. Ahmad Z, Wang S, Mark JE (1993) Polym Prepr (ACS Div Polym Chem) 34:745
14. Ahmad Z, Sarwar MI, Mark JE (1997) J Mater Chem 7:259
15. Ahmad Z, Sarwar MI, Mark JE (1997) J Appl Polym Sci 63:1345
16. Ahmad Z, Sarwar MI, Wang S, Mark JE (1997) Polymer 38:4523
17. Ahmad Z, Sarwar MI, Mark JE (1998) J Appl Polym Sci 70:297
18. Rehman HU, Sarwar MI, Ahmad Z, Krug H, Schmidt H (1997) J Non-Cryst Solids 211:105
19. Ahmad Z, Sarwar MI, Krug H, Schmidt H (1997) Die Angew Makromol Chemie 248:139
20. Ahmad Z, Sarwar MI, Krug H, Schmidt H (1998) Intern J Polym Mater 39:127
21. Wang S, Ahmad Z, Mark JE (1994) Polym Mater Sci Eng 70:305
22. Wang S, Ahmad Z, Mark JE (1994) Macromolecular Reports 31:411
23. Ahmad Z, Wang S, Mark JE (1994) Polym Mater Sci Eng 70:425
24. Wang S, Ahmad Z, Mark JE (1994) Chem Mater 6:943
25. Ahmad Z, Wang S, Mark JE (1994) Polym Mater Sci Eng 70:303
26. Chen JP, Ahmad Z, Wang S, Mark JE, Arnold FE (1995) ACS Symp Ser 585:297
27. Ahmad Z, Wang S, Mark JE (1995) ACS Symp Ser 585:291
28. Rodrigues DE, Brennan AB, Betrabet C, Wang B, Wilkes GL (1992) Chem Mater 4:1437
29. Mascia L, Kioul A (1994) J Mater Sci Lett 13:641
30. Kakimoto M, Iyoku Y, Morikawa A, Yamaguchi H, Imai Y (1994) Polym Prepr (ACS Div Polym Chem) 35:393
31. Asif KM, Sarwar MI, Rafiq S, Ahmad Z (1998) Polym Bull 40:583
32. Zulfiqar S, Ahmad Z, Ishaq M, Saeed S, Sarwar MI (2007) J Mater Sci 42:93
33. Kausar A, Zulfiqar S, Shabbir S, Ishaq M, Sarwar MI (2007) Polym Bull (in press)
34. Sarwar MI, Zulfiqar S, Ahmad Z (2007) Polym Int 56:000
35. Sarwar MI, Zulfiqar S, Ahmad Z (2007) J Sol Gel Sci Technol (in press)
36. Strong AB (1996) Plastics: materials and processing. Prentice-Hall, NJ
37. Trostyanskaya EB (1995) In: Shain RE (ed) Polymer matrix composites. Chapman and Hall, London
38. Preston J, Dobinson F (1964) Polym Letters 2:1175
39. Brennan AB, Wilkes GL (1991) Polymer 32:733